Astrophys Space Sci (2015) 355:95–103
DOI 10.1007/s10509-014-2149-7

ORIGINAL ARTICLE

A comprehensive comparative study of temporal properties between X-ray flares and GRB pulses

Z.Y. Peng · Y. Yin · T.F. Yi · Y.Y. Bao · H. Wu

Received: 22 July 2014 / Accepted: 17 September 2014 / Published online: 4 December 2014

Abstract We demonstrate that the optical flares, X-ray flares (XRFs), and the gamma-ray burst (GRB) pulses exhibit similar behaviors as evidenced by correlations among temporal properties and the temporal properties on energy by a comprehensive comparative analysis of 24 optical flares, 92 XRFs and 102 GRB pulses. The flare/pulse peak time, t_{pk}, is correlated with their width, w, and with w/t_{pk} for the three samples, but their slopes are very different. Both of the flares and GRB pulses bear the similar asymmetries and the asymmetry evolves neither with w nor with t_{pk}. The spectral lags of the XRFs are much larger than those of the GRB pulses and almost follow the same lag versus width relation as that of the GRB pulse. In addition, the corresponding broadening of temporal properties (width, rise width and decay width) of the XRFs with energy decreasing follows the same power-law relation as those of the GRB pulses. The K-S tests show the distributions of the three corresponding power-law indices of the XRFs are the same as those of the GRB pulses at the 1 % significance level. All of our demonstrated relations and previous correlated relations seem to indicate that the XRFs as well as the optical flares should be belong to a extended class of the prompt GRBs that dominate the tail of the distribution function. Therefore, our analysis results place some constraints on the physical mechanism responsible for the pulsed emission properties.

Keywords Gamma rays: bursts · Method: statistical

1 Introduction

One of the most intriguing contributions of the Swift Mission is the detection of flares in the observed gamma-ray burst (GRB) afterglows. Until now more than 50 % of the GRBs observed with the Swift XRT have found early-time flares, which were observed at the end of the prompt emission and/or the early afterglow phase. While some late-time X-ray flares (XRFs) were observed at even several days after the prompt emission. The flares were found superimposed to short and long bursts, low and high redshift X-ray afterglow light curve (Burrows et al. 2005; Falcone et al. 2006, 2007; Chincarini et al. 2007). Due to these phenomena give information about the activity of the central engine they drawn much observational and theoretical attention. As a result a lot of theoretical speculations have been proposed to explain it. The rapid rise and decay behavior of X-ray flares is widely understood as being due to some long-lasting activity of the central engines and widely believed to be associated with the later activation of central engine. Burrows et al. (2005) proposed that the flares are produced in internal shocks at later times, which requires reactivation of the GRB central engine. Similar conclusions have been also drawn by other authors (e.g. Ioka et al. 2005; Fan et al. 2005; Zhang et al. 2006; Falcone et al. 2006; and Romano et al. 2006; Maxham and Zhang 2009; Wang and Dai 2013). While Piro et al. (2005) and Galli and

Z.Y. Peng (✉) · T.F. Yi · H. Wu
College of Physics and Electronics, Yunnan Normal University, Kunming 650500, P.R. China
e-mail: pengzhaoyang412@163.com

H. Wu (✉)
e-mail: 1286328153@qq.com

Y. Yin
Department of Physics, Liupanshui Normal College, Liupanshui 553004, P.R. China

Y.Y. Bao
Department of Physics, Yuxi Normal College, Yuxi 653100, P.R. China

Piro (2006) showed that X-ray flares may be produced by a delayed external shock. Wu et al. (2005) suggested that some X-ray flares originate from late external shock but some arise from internal shock by performing a quantitative analysis in the context of late external shock and late internal shock models. Therefore, the underlying mechanisms that produce the flaring activity are not fully understood.

It is generally believed that GRB prompt emission originates from the internal shock model (Meszaros and Rees 1997; Kobayashi et al. 1997; Daigne and Mochkovitch 1998). While the broadband afterglows are produced by the external shocks when the fireball is decelerated by the ambient medium (Meszaros and Rees 1997; Sari et al. 1998). This internal + external shock model suggests that the prompt emission and the afterglow involve two distinct processes at two different emission sites. In order to understand the underlying mechanisms of the flaring activity one of the main questions is that both the flare activity and prompt emission share the same internal shock mechanism? The question focus primarily on the linking the observed temporal and spectral properties of prompt emission in long bursts to similar properties seen in bursts exhibiting XRFs. Some authors studied the X-ray flare and prompt emission pulses in GRBs and revealed many similarities between them during the fast decay and afterglow phases of GRBs, which seems to suggest the strong indications that X-ray flares have a common origin with the gamma-ray pulses. These examples include: (1) the extending lag-luminosity relation to X-ray flares (Margutti et al. 2010); (2) the spectra of flares are better fitted by the standard fitting model for GRB prompt emission (Band function) than by a standard afterglow model (an absorbed power law) (Falcone et al. 2006); (3) the spectral properties of flares harder than underlying afterglow and follow the hard-to-soft spectral evolution; (4) studies of evolution of spectral lag; and (5) the flare fluence can be up to the prompt fluence. Furthermore, the presence of an underlying continuum with the same slope before and after the flaring activity excludes the possibility that flares are related to the afterglow emission by forward external shocks. Therefore their properties can provide an important clue towards the understanding of the mechanism that is at the basis of the GRB phenomenon.

Some evidences showed by Li et al. (2012) that the temporal properties of the optical flares is also similar to the XRFs and the GRB pulses. For example, the optical and the XRFs as well as the GRB pulses follow the same pulse width (w) versus the peak time (t_p) relation. In addition, the observed relations between either E_{iso} or L_{iso} and t_p also followed by the X-ray and optical flares.

The widthes of the GRB pulses are found to be energy dependent, i.e., the higher energies, the narrower widthes (e.g., Link et al. 1993). In addition, the pulse width dependence on energy is a power law (e.g., Fenimore et al. 1995; Norris et al. 1996, 2005; Nemiroff 2000; Crew et al. 2003; Peng et al. 2006). Moreover, it is found that this power-law relation can be extended to X-ray bands (see, Zhang and Qin 2008; Zhang 2008) as well as the XRFs (e.g. Chincarini et al. 2010). In addition, Zhang et al. (2007) showed that the pulse peak time, rise time scale, and decay time scale on energy are also power-law functions.

Recently, Chincarini et al. (2010, hereafter Paper I) studied the evolution of the flare temporal properties with energy in different X-ray energy bands using an updated catalogue of 113 X-ray flares detected by Swift. Margutti et al. (2010) also investigated the temporal properties with a small sample including 9 light X-ray flares. Some important conclusions were drawn about the temporal properties of flare by their work. But Paper I and Margutti et al. (2010) did not systematically compare their temporal properties with GRB pulse. While two recent work by Peng et al. (2012, 2013) investigated the temporal properties on energy of some GRB pulses with a large sample. In this work we aim to perform a comprehensive comparative analysis of the temporal properties of the XRFs, the optical flares and the GRB pulses to further reveal their possible relations. Our paper is organized as follows. In Sect. 2, we present the sample description and pulse modeling. The analysis and results are given in Sect. 3. Conclusions and discussion are presented in the last section.

2 Sample description and pulse modeling

In this study, we select three samples to perform the comparative analysis of the temporal properties between the XRFs, optical flares and GRB pulses. The first sample comes from Paper I, consisting of 113 well-separated early-time X-ray flares (the peak time less than 1000 s) with a relatively complete structure and clearly distinguishable from the underlying continuum. These flares mainly from the X-ray afterglows observed by Swift XRT between 2005 April and 2008 March. The flare structure can be fitted with an analytic function, thus giving a homogeneous set of parameters. For a full description of the data reduction we can refer to Paper I. The second sample consisting of 102 "clean" GRB pulses is from Peng et al. (2013), which were observed by CGRO/BATSE with durations longer than 2 s. In fact, the sample was composed of three GRB samples compiled by Kocevski et al. (2003), Norris et al. (1999) and Norris et al. (2005). The bursts of the first BATSE sample including 76 individual pulses in 67 bursts are found to contain individual FRED pulses with the peak flux is greater than 1.0 photon $\mathrm{cm}^{-2}\,\mathrm{s}^{-1}$ on a 256 ms time-scale. The second BATSE sample coming from Norris et al. (1999) contains 66 single-pulse GRBs. The third BATSE sample containing 35 pulses is a long-lag wide pulse burst sample with an average lag > 1 s and $F_{peak} > 0.75$ photons $\mathrm{cm}^{-2}\,\mathrm{s}^{-1}$ (50–300 keV).

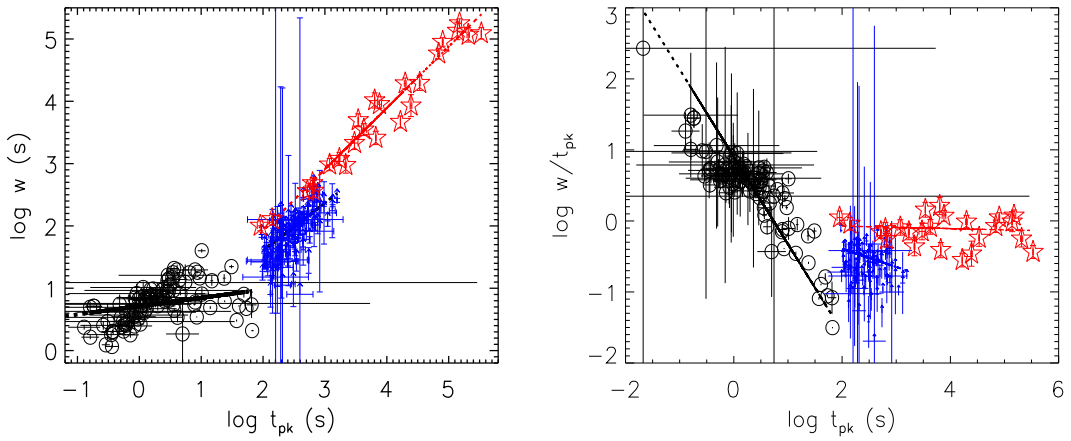

Fig. 1 The observed width (*left panel*) as well as the relative variability time-scale (w/t_{pk}) (*right panel*) versus the observed peak time for the optical flares (*red five stars*), X-ray flares (*blue arrows*), and GRB pulses (*black circles*)

These long-lag pulses are sufficiently non-overlapping to allow pulse fits with negligible ambiguity. (For further information about the samples, see Kocevski et al. 2003 and Norris et al. 1999, 2005.) The third sample containing 24 optical flares comes from Li et al. (2012). They first compiled a sample of 225 optical light curves in the literature. Then they made an extensive search for the optical data from published papers or from GCN Circulars and obtained well-sampled light-curves from 146 GRBs. They fitted the light-curves with a power-law function or a smooth broken power-law function or a smooth triple power-law function to separate the different components from the optical light-curves. Finally, they got 24 optical flares in 19 GRBs. Most of the flares are in R band while they corrected them to R band with the optical spectral indices for the flares in other bands. The temporal properties (the peak time, the width measured at the full width at half-maximum, the rising timescale, the decay timescale) were derived from the fitting parameters.

In order to investigate the pulse temporal properties, both of the X-ray flarse and GRB pulses are modeled with the empirical functional pulse form of Norris et al. (2005):

$$I(t) = A\lambda \exp\left[-\tau_1/(t-t_s) - (t-t_s)/\tau_2\right], \quad (1)$$

where t is time since trigger, A is the pulse amplitude, t_s is the pulse start time, τ_1 and τ_2 are characteristics of the pulse rise and pulse decay, and the constant $\lambda = \exp[2(\tau_1/\tau_2)^{1/2}]$.

According to the fitting parameters we can obtain the measured pulse temporal properties including the pulse width $w = \Delta\tau_{1/e} = \tau_2(1+2\ln\lambda)^{1/2}$, the pulse asymmetry, $k = \tau_2/w$, the pulse rise width, $\tau_{rise} = \frac{1}{2}w(1-k)$, and the decay width $\tau_{decay} = \frac{1}{2}w(1+k)$. The pulse peak times are given by $t_{pk} = t_{eff} + \sqrt{\tau_1\tau_2}$.

3 Analysis and results

In this section, we mainly want to compare the temporal properties of the X-ray flares, the optical flares with those of the GRB pulses. Following Paper I we consider the parameters of the XRFs (GRB) pulses obtained from the 0.3–10 (25–1800) keV band light curve when not specified. While the optical flares are considered in R band.

3.1 The comparison of the temporal properties of X-ray flares, optical flare and GRB pulses

In this section, let us first analyze in detail the temporal properties of the observables, pulse peak time, pulse width, pulse rise time, pulse decay time, pulse asymmetry, and pulse peak lag. The temporal properties of the optical flares, XRFs, and GRB pulses examined in this study exhibit many similarities; these can be demonstrated in the following sections.

3.1.1 W and t_{pk}

Showed in the Fig. 1 (left panel) is the scatter plot between pulse width and pulse peak time for the three samples. A strong positive correlation exists between the pulse width and the pulse peak time; this correlation is present for both flares and GRB pulses (see, Fig. 1 and Table 1). These show that the width evolves linearly with time to larger values, which is very similar to the result of Li et al. (2012) (see, Fig. 5 in their paper). However, the slopes of the optical flares (0.98) and the XRFs (0.77) are much larger than that of the GRB pulses (0.13) (see, Table 1). This result is slightly different from that of Paper I and Ramirez-Ruiz and Fenimore (2000), which showed that the width of GRB pulses remain constant throughout the GRB time history.

Figure 1 (right panel) also illustrates the relative variability time-scale (w/t_{pk}) versus peak time. An opposite

Table 1 The correlations and regression coefficients of the width along with the ratio of width to the peak time and the peak time for the GRB pulses (G), XRFs (X) and optical flares (O)

Parameter pairs	R_S	P_S	a	b
$(w - t_{pk})_G$	0.57	7.26×10^{-10}	0.71 ± 0.01	0.13 ± 0.00
$(w - t_{pk})_X$	0.71	6.46×10^{-18}	0.07 ± 0.03	0.77 ± 0.03
$(w - t_{pk})_O$	0.99	5.23×10^{-20}	-0.20 ± 0.11	0.98 ± 0.04
$(w/t_{pk} - t_{pk})_G$	0.78	2.34×10^{-21}	0.90 ± 0.01	-1.23 ± 0.01
$(w/t_{pk} - t_{pk})_X$	−0.12	0.19×10^{0}	0.12 ± 0.01	-0.26 ± 0.03
$(w/t_{pk} - t_{pk})_O$	−0.04	0.84×10^{0}	-0.20 ± 0.11	-0.02 ± 0.04

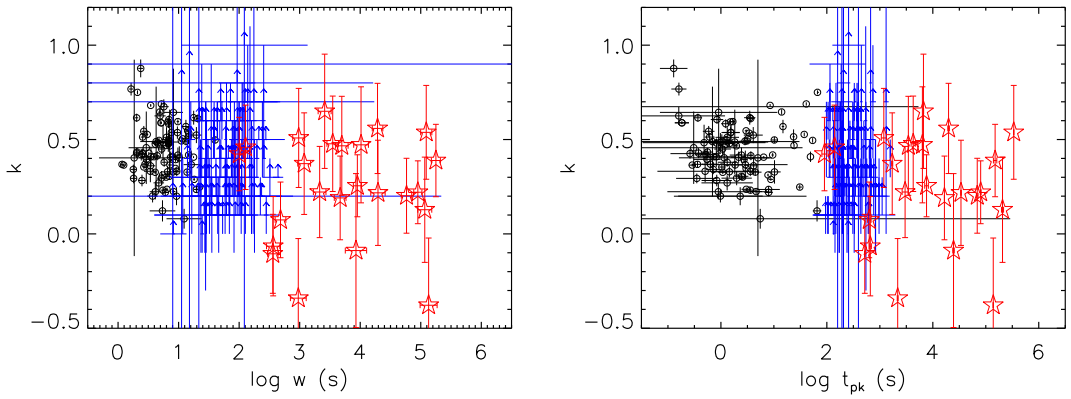

Fig. 2 Asymmetry versus width (*left panel*) as well as asymmetry versus peak time (*right panel*) for the optical flare (*red five stars*), X-ray flare (*blue arrows*) and GRB pulse (*black circles*)

evolutionary trend is demonstrated when compared with w versus t_{pk}. The w/t_{pk} of the GRB pulses decrease sharply with peak time, $slope = -1.23$, the XRFs decrease much slower ($slope = -0.26$) and the optical flares tends to remain constant ($slope = -0.02$) up to late times (see, Fig. 1 and Table 1). Though there are two different trends of w and w/t_{pk} with time for flares and GRB pulses they can connect smoothly each other.

3.1.2 Asymmetry and t_{pk}

Figure 2 demonstrates the relationship between asymmetry and width as well as between asymmetry versus peak time, respectively. No correlated trend for the three samples are found but their statistical uncorrelation also joined by optical flare, X-ray flares and GRB pulses. The uncorrelation of asymmetry and peak time is not in agreement with the tentative anti-correlated trend revealed by Norris et al. (2005) with a long-lag wide GRB pulse sample.

Figure 3 further demonstrates that both of the flares (X-ray and optical) and the GRB pulses have strong correlations between rise and decay time scales. The correlation connects smoothly from the prompt GRB pulses through optical flares. Moreover, their slopes are very close.

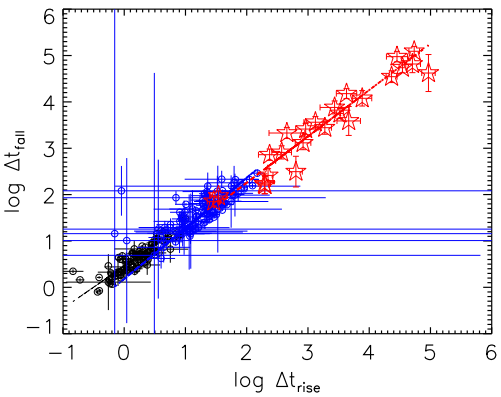

Fig. 3 The plot of decay times versus rise times for the optical flares (*red five stars*), the XRFs (*blue arrows*), and the GRB pulses (*black circles*)

3.1.3 W and peak lag

The strong correlation between the pulse width and the spectral lag for the GRB pulses was found by several authors (e.g. Norris et al. 2005; Peng et al. 2007; Hakkila et al. 2008). That is, the spiky pulses have shorter lags than broad pulses. Whether the correlation exists in the X-ray flare or not? This has also been done by Margutti et al. (2010) with a sample including 9 bright X-ray flares. We recheck the relation with a much larger sample. Some theories predict that the lag is highly dependent on energy (e.g. Shenoy et al.

2013), implying that the choice of energy channels is important and should be made carefully. We have defined our lags so that they span a reasonably large spectral range, and also in terms of large signal-to-noise, so that they encompass a large amount of the GRB pulse's or flare's total flux. For BATSE, these conditions are generally met by selecting channel 1 (25 to 50 keV) and channel 3 (100 to 300 keV), while for the Swift XRT most of these conditions are met by choosing Swift XRT channel 1 and channel 3. We assume that this allows us to compare GRB pulse properties to XRF properties in principle, lacking data to the contrary. Peak lag Δt_{13} can be obtained between energies of 2–3 keV (XRT channel 3) and the 0.3–1 keV (XRT channel 3) for any XRF. For the sake of comparison we also find the peak lag between energies of 100–300 keV (BATSE channel 3) and 25–50 keV (BATSE channel 1) for any GRB pulse. Figure 4 illustrates the scatter plot of the width versus the peak lag for the XRFs and GRB pulses. Similar to the GRB pulse the important lag versus width correlation also exists in XRFs and their evolution slope of Δt_{13} versus w (see, also Table 2) is very close to that of the GRB pulse. However, not all flare lags are positive; this is very similar to the GRB pulse lags. The correlation of the XRFs also connects smoothly with the GRB pulses.

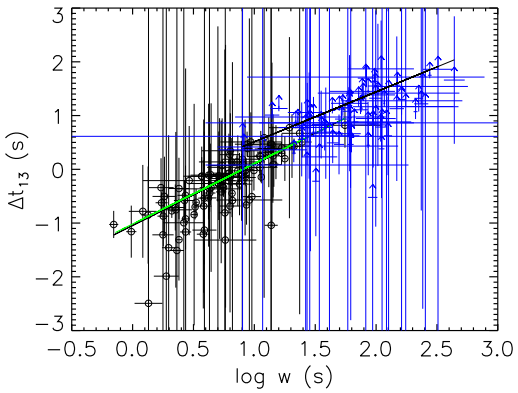

Fig. 4 The relation between the peak lag and the width of the XRFs (*blue arrows*) and the GRB pulses (*black circles*)

Table 2 The correlations and regression coefficients of the width and the peak lag for the GRB pulses and the XRFs

Parameter pairs	R_S	P_S	a	b
$(w-\Delta t_{13})_P$	0.70	2.70×10^{-16}	-1.04 ± 0.10	1.14 ± 0.10
$(w-\Delta t_{13})_X$	0.43	8.32×10^{-5}	-0.42 ± 0.11	0.93 ± 0.05

3.1.4 *Intensity and t_{pk}*

A evident correlation between the intensity and t_{pk} exists for the early-time flares is identified by Paper I and Chincarini et al. (2007). Using the optical flare data we also find the same correlated relation exists. For the GRB pulses, however, the situation is very different; the intensity almost remain constant with the variation of the peak time. Thus there has no correlation between intensity and peak time with correlation coefficient $r = 0.15$ and possibility $p = 0.13$ (see Fig. 5). However, the very strong correlation and the similar evolutionary trends between the intensity and the width exist for all of the three samples (see Fig. 5).

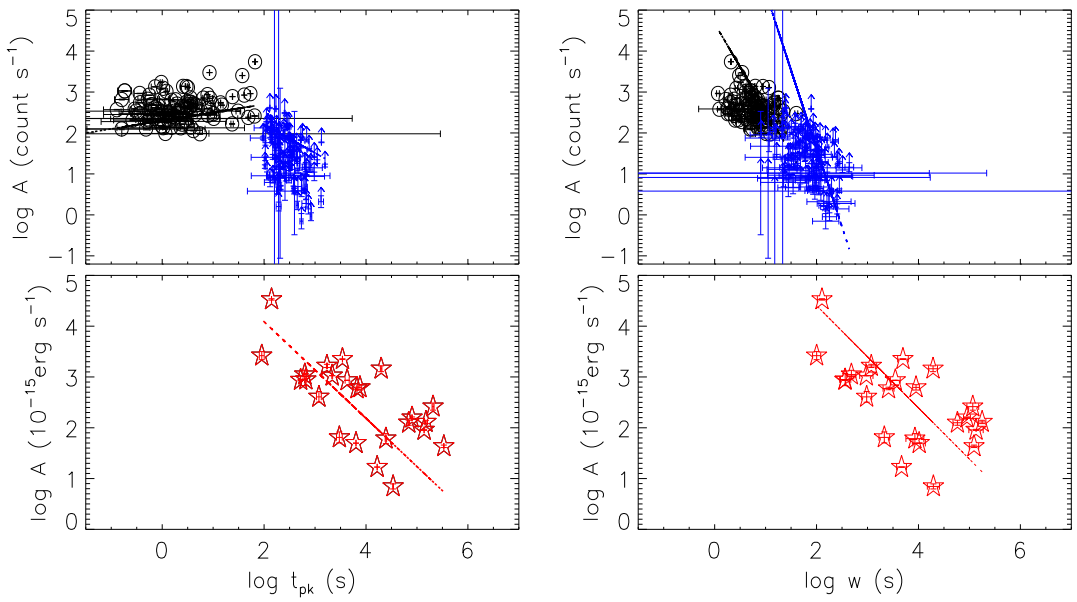

Fig. 5 Plots of the peak intensity versus the peak time (*left panel*) as well as the peak intensity versus the width (*right panel*) for the optical flares (*red five stars*), the XRFs (*blue arrows*), and the GRB pulses (*black circles*)

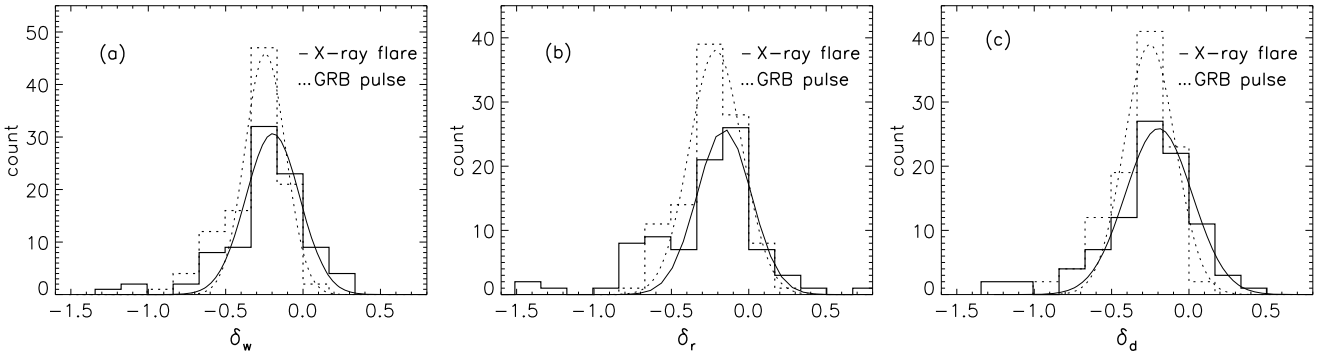

Fig. 6 Histograms of the power-law indices δ_w (**a**), δ_r (**b**), and δ_d (**c**) obtained by fitting the pulse width, rise width, and decay width and energy with a power-law function, respectively. The *curved lines* are the best fits by the Gaussian functions

Table 3 A list of the distribution parameters of the three power-law indices of the XRFs (X) and the GRB pulses (G)

Power-law indices	Mean	Median	σ (modeled with a Gaussian profile)
δ_{w_X}	−0.25	−0.21	-0.19 ± 0.18
δ_{w_G}	−0.30	−0.25	-0.24 ± 0.13
δ_{r_X}	−0.26	−0.19	-0.16 ± 0.18
δ_{r_G}	−0.25	−0.23	-0.21 ± 0.17
δ_{d_X}	−0.26	−0.22	-0.19 ± 0.22
δ_{d_G}	−0.32	−0.27	-0.25 ± 0.16

3.2 The comparison of the temporal properties on energy between X-ray flares and GRB pulses

In this section, we compare the temporal properties on energy between the XRFs and the GRB pulses since the power law relation between the pulse width and energy exists in the GRB pulses and extend to the XRFs. By fitting the widthes, rise widthes, and decay widthes of the XRFs and the GRB pulses (in the logarithm) per channel as a function of the geometric means of the lower and upper XRT and BATSE channel boundaries (using 300–1000 keV for BATSE channel 4; Norris et al. 2005) the power-law indices are thus obtained (let δ_w, δ_r, and δ_d, denotes the indices of the power-law relations between w, τ_{rise}, and τ_{decay} and energy, respectively). Therefore, the dependencies of the three temporal quantities on energies can be parameterized by the power-law indices.

Displayed in Fig. 6 are the histograms of the three power-law indices of temporal properties on energy. The distribution parameters are listed in Table 3. From Fig. 6 and Table 3 we find that the corresponding distributions of these indices share similar widthes but all of them have large dispersions. In addition, the indices of X-ray flares have a slightly smaller values and with larger dispersions than that of the GRB pulses. The large dispersions imply that the energy dependence of the temporal properties may not be the same for different bursts or flares. In order to further compare the dependence of temporal properties on energy between the XRFs and the GRB pulses we do the Kolmogorov–Smirnov (K-S) test (Press et al. 1992) to check if the distributions of these indices are the same. The K-S test determines the parameter $D_{K\text{-}S}$, which measures the maximum difference in the cumulative probability distributions over parameter space, and the significance probability $P_{K\text{-}S}$ for the value of $D_{K\text{-}S}$. A small $P_{K\text{-}S}$ indicates that the data sets are likely to be different (Press et al. 1992). The results of the K-S tests are listed in Table 4. It is found that we can not reject the null hypothesis at the 1 % significance level for all of the three cases. Even at the 5 % significance level we can not reject the null hypothesis for the case of δ_r. Therefore, there are not enough reasons to believe that the dependence of temporal properties on energy may be different between the XRFs and the GRB pulses. In other words, the dependencies of pulse widthes, rise widthes, and decay widthes on energies is the same as that the flare widthes, rise widthes, and decay widthes on energies, respectively, even if the energies are much different.

Table 4 The results of the K-S test for the three power-law indices of the XRFs and the GRB pulses

Power-law indices	$D_{K\text{-}S}$	$P_{K\text{-}S}$
δ_w	0.21	0.03
δ_r	0.16	0.14
δ_d	0.20	0.04

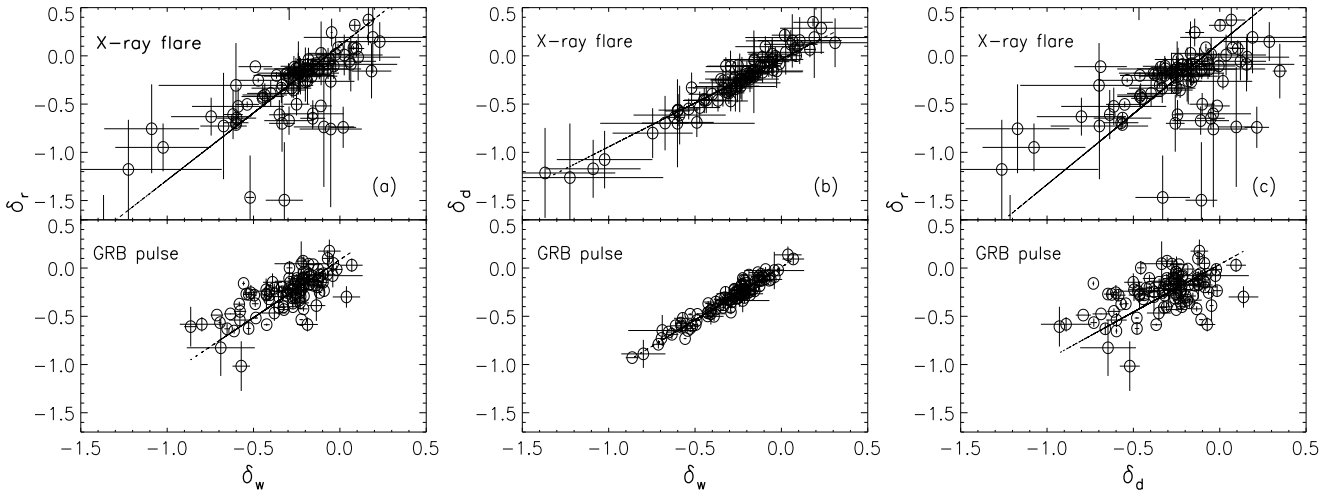

Fig. 7 Relationships of the three power-law indices δ_r vs. δ_w (**a**), δ_d vs. δ_w (**b**), δ_r vs. δ_d (**c**). The *dashed lines* are the regression lines

Table 5 Correlations and the regression coefficients of the three power-law index pairs for the XRFs (X) and GRB pulses (G)

Power-law indices	R_S	P_S	a	b
$(\delta_r - \delta_w)_X$	0.70	1.01×10^{-14}	0.10 ± 0.02	1.39 ± 0.06
$(\delta_r - \delta_w)_G$	0.68	2.05×10^{-15}	0.09 ± 0.01	1.20 ± 0.02
$(\delta_d - \delta_w)_X$	0.94	3.64×10^{-43}	-0.03 ± 0.02	0.91 ± 0.03
$(\delta_d - \delta_w)_G$	0.94	0.00×0.00	0.01 ± 0.00	1.10 ± 0.01
$(\delta_r - \delta_d)_X$	0.49	1.04×10^{-6}	0.13 ± 0.02	1.47 ± 0.07
$(\delta_r - \delta_d)_G$	0.44	2.83×10^{-6}	0.04 ± 0.01	0.99 ± 0.02

Peng et al. (2012) have examined the relationships between the three power-law indices, δ_w, δ_r, and δ_d by using a single GRB pulse sample and found that the three power-law indices are strongly correlated with each other. We also check whether the correlations exist in the XRFs or not. Figure 7 shows the relationships between the three indices along with those of the GRB pulses. The Spearman rank-order correlation analysis of the three quantities as well as the regression coefficients a (intercept), b (slope) are listed in Table 5. It is revealed that the correlations are also exist in the XRFs, which also strongly indicates that the temporal properties (the rise times and the decay times) of the XRFs do not evolve independently from each other; instead, their evolution is tightly coupled. Similar to GRB pulses the correlation between δ_w and δ_d is much stronger than the other two index pairs and the two indices may be viewed as mutual surrogates for the XRFs. Moreover, the corresponding correlation and regression coefficients of index pairs are also close to each other for the X-ray flare and the GRB pulses (see, Fig. 7 and Table 5).

4 Conclusions and discussion

In this paper, we have selected a XRF sample containing 92 early-time flares, a optical flare sample consisting of 24 flares and a GRB pulse sample including 102 well-separated long-duration GRB pulses and analyzed their temporal properties as well as temporal properties on energy with the aim to search for their connections.

We first perform the comparative analysis of the width versus the peak time, which supports the known result that the width would be increase with the decreasing energy and the general trend is that later flares or pulses tend to be wider (see, Fig. 1) when we combine the flares (X-ray and optical) with GRB pulses. The temporal evolution of the width from the GRB pulses to the optical flare phase reveals the global evolution of the erratic GRB central engine. Maxham and Zhang (2009) pointed out that this demands that the central engine is ejecting thicker and dimmer shells at late times instead of the hydrodynamical spreading of the shells ejected at late times. Another possible interpretation is that the late flares being produced by clumps at larger radii, and the spreading during the accretion process would increase the accretion time onto the black hole (Perna et al. 2006; Proga and Zhang 2006). However, the evolutional slopes of width with time would be different in the different phase (see, Fig. 1).

The comparison of the relative variability time-scale $\Delta t/t$ shows the prompt emission pulses with very large dispersion are very different from those flares. Most of them is

larger than 1 only a few overlapping with the flares. Whereas all of the optical and X-ray flare is less than 1 and they overlap each other even their central values are different (see, Fig. 1). However, Swenson et al. (2013) analyzed 119 ultraviolet/optical flares and found that $\Delta t/t$ vary from 0.01 to greater than 10, with about 8 % of the flares exhibiting a $\Delta t/t > 1$. If we consider the late X-ray flare there exist flares with $\Delta t/t > 1$ (Bernardini et al. 2011). These seem to show that $\Delta t/t$ of the flares and the GRB pulses overlap each other. Therefore, if only considering the relative variability time-scale we can not discriminate among different models.

The analysis of the asymmetries of the three samples shows that the optical flares and the XRFs are more asymmetry than the GRB pulses. We also found no correlation between width and asymmetry as well as width and peak time for all of the three samples. Moreover, the linear evolution of the decay time as a function of the rise time is presented in the three samples and is valid over 5 orders of magnitude. These strongly indicate that the rise and the decay times of the flares and pulses do not evolve independently from one another; instead, their evolution is tightly coupled.

Similar to the GRB pulses a interesting correlated relation between the width and peak lag for the XRFs is also revealed. Moreover, their slope of the two quantities for the X-ray flare and GRB pulse is close (see, Fig. 4 and Table 2). The statistical result also show that their origin may be the same.

A striking similarity is revealed by analyzing the temporal properties (widthes, rise widthes and decay widthes) on energies for the XRFs and the GRB pulses even if the energies are very different. First, the strong correlations between the three power-law indices also exist for the XRFs, which also strongly indicates that the rise and the decay times of the XRFs do not evolve independently from each other. Second, the distributions of the corresponding power-law indices for XRFs and GRB pulses are very similar and all of them have a large dispersion. These imply that the energy dependence of the temporal properties may not be the same for different flares or pulses. Moreover, the correlation and regression coefficients of the corresponding indices is also close to each other for XRFs and GRB pulses. It is clear that the power-law indices of the temporal properties on energy are caused by the pulse widening with energy. But the origin of the pulse widening has not been interpreted completely. Maybe the kinematic effect plays an important role on the pulse widening and the correlated relations. Some studies (e.g., Ioka and Nakamura 2001; Qin et al. 2005; Willingale et al. 2010; Peng et al. 2012) support the kinematic origin.

Other similarity between the XRFs and the GRB pulses are also shown by many studies. For example, the important lag-luminosity relation for the XRFs is revealed by Margutti et al. (2010), which follows the same evolutionary trend as the prompt GRB pulses (see, Fig. 4 in their paper). The peak luminosity versus rest-frame width correlation was shown by Paper I. This means that short-lag flares have shorter durations are more luminous than those of longer flares. This property is consistent with that of the prompt GRB pulse first found by Hakkila et al. (2008). Sonbas et al. (2013) compared the variability time scale with pulse parameters such as rise times, spectral lags, and revealed a tight correlation between these temporal features for both of the XRFs and the GRB pulses (see, Figs. 3 and 4 in their paper). The observed correlated relations exist between isotropic gamma-ray energy and isotropic optical flare energy as well as the optical flare luminosity and the gamma-ray luminosity; these indicate that the prompt gamma-ray emission and later optical flare emission could have the same physical origin (Li et al. 2012).

Combined with above-mentioned analysis results we tend to believe that the XRFs should be belong to the extend class of GRB with less energies. While the optical flare is also a possible extend class of GRB with much less energies. These also suggest a direct link between the physical mechanisms that lead to produce the flares and prompt emission in GRBs and place some constraints on the physical mechanism responsible for the pulsed emission properties.

The similarity of flare and prompt emission pulse can be interpreted by the internal shock model in which the basic emission units are assumed to be pulses that are produced via the collision of relativistic shells emitted by the central engine. Many works support the pulse paradigm view of the prompt emission in GRBs (e.g. Hakkila et al. 2008; Hakkila and Cumbee 2009; Hakkila and Preece 2011; Bhat et al. 2012). Maxham and Zhang (2009) used the internal shell collision model to explain the major temporal features of the XRFs. Moreover, they pointed out that the XRF time history reflects the time history of the central engine, and reactivates multiple times after the main prompt emission phase. The internal collisions producing flares occur in the same conditions as those producing the prompt emission pulses (Lazzati and Perna 2007). The differences observed in flares and the prompt emission pulses only depend on the intrinsic differences in the shells ejected by the central engine (Maxham and Zhang 2009). The flares corresponds to less energetic shells ejected at late time from central engine (Lazzati et al. 2008).

There are also some evidences show the differences between the prompt emission pulses and the flares. For example, an evident difference between them is that the relative variability time-scale $\Delta t/t$ of the flares almost constant with peak time (see Fig. 1). This is not expected for the internal shock model since the arrival time is not related to the conditions of the collision (see, e.g. Kobayashi et al. 1997; Ramirez-Ruiz and Fenimore 2000) and in fact this is not

found in prompt emission pulses. Chincarini et al. (2007) found there has no correlation between the characteristics of the prompt emission as observed by BAT and the frequency of flares detected by XRT. Swenson et al. (2013) also compared the UV/optical flare parameters with prompt emission parameters, T_{90}, fluence, and the amount of structure presented in the prompt emission to T_p, $\Delta t/t$, the flux ratio and the number of flares per GRB. They found no correlations between any of the prompt emission parameters and flare parameters. The lack of correlation seems to indicate that the emission source of the flares detected is not the same as that of the high energy prompt GRB emission.

Acknowledgements We acknowledge the anonymous referee for careful and helpful review. We thank Xiaohong Zhao for helpful discussions. This work was supported by the National Natural Science Foundation of China (grant 11263006), the Key Program for Science Fund of the Education Department of Yunnan Province (2011Z004), the Open Research Program of Key Laboratory for the Structure and Evolution of Celestial Objects (OP201106), the High-Energy Astrophysics Science and Technology Innovation Team of Yunnan Higher School and the Yunnan Gravitation Theory Innovation Team (2011C1).

References

Bernardini, M.G., et al.: Astron. Astrophys. **526**, 27 (2011)
Bhat, P.N., et al.: Astrophys. J. **744**, 141 (2012)
Burrows, D.N., et al.: Science **309**, 1833 (2005)
Chincarini, G., et al.: Astrophys. J. **671**, 1903 (2007)
Chincarini, G., et al.: Mon. Not. R. Astron. Soc. **406**, 2113 (2010) (Paper I)
Crew, G.B., et al.: Astrophys. J. **599**, 387 (2003)
Daigne, F., Mochkovitch, R.: Mon. Not. R. Astron. Soc. **296**, 275 (1998)
Falcone, A.D., et al.: Astrophys. J. **641**, 1010 (2006)
Falcone, A.D., et al.: Astrophys. J. **671**, 1921 (2007)
Fenimore, E.E., et al.: Astrophys. J. **448**, L101 (1995)
Fan, Y.Z., Zhang, B., Proga, D.: Astrophys. J. **635**, L129 (2005)
Galli, A., Piro, L.: Astron. Astrophys. **455**, 413 (2006)
Hakkila, J., et al.: Astrophys. J. **677**, L81 (2008)
Hakkila, J., Cumbee, R.S.: In: Meegan, C., Kouveliotou, C., Gehrels, N. (eds.) AIP Conf. Proc 1133, Gamma-Ray Burst. Am. Inst. of Phys., New York (2009)
Hakkila, J., Preece, R.D.: Astrophys. J. **740**, 104 (2011)
Ioka, K., Nakamura, T.: Astrophys. J. **554**, L163 (2001)
Ioka, K., Kobayashi, S., Zhang, B.: Astrophys. J. **631**, 429 (2005)
Kobayashi, S., Piran, T., Sari, R.: Astrophys. J. **490**, 92 (1997)
Kocevski, D., Ryde, F., Liang, E.: Astrophys. J. **596**, 389 (2003)
Lazzati, D., Perna, R.: Mon. Not. R. Astron. Soc. **375**, L46 (2007)
Lazzati, D., Perna, R., Begelman, M.C.: Mon. Not. R. Astron. Soc. **388**, L15 (2008)
Li, L., et al.: Astrophys. J. **758**, 27 (2012)
Link, B., Epstein, R.I., Priedhorsky, W.C.: Astrophys. J. **408**, L81 (1993)
Maxham, A., Zhang, B.: Astrophys. J. **707**, 1623 (2009)
Margutti, R., et al.: Mon. Not. R. Astron. Soc. **406**, 2149 (2010)
Meszaros, P., Rees, M.J.: Astrophys. J. **482**, L29 (1997)
Nemiroff, R.J.: Astrophys. J. **544**, 805 (2000)
Norris, J.P., et al.: Astrophys. J. **459**, 393 (1996)
Norris, J.P., Bonnell, J.T., Watanabe, K.: Astrophys. J. **518**, 901 (1999)
Norris, J.P., et al.: Astrophys. J. **627**, 324 (2005)
Peng, Z.Y., et al.: Mon. Not. R. Astron. Soc. **368**, 1351 (2006)
Peng, Z.Y., et al.: Chin. J. Astron. Astrophys. **7**, 428 (2007)
Peng, Z.Y., et al.: Astrophys. J. **752**, 132 (2012)
Peng, Z.Y., et al.: Publ. Astron. Soc. Jpn. **65**, 71 (2013)
Perna, R., Armitage, P.J., Zhang, B.: Astrophys. J. **636**, L29 (2006)
Piro, L., et al.: Astrophys. J. **623**, 314 (2005)
Press, et al.: Numerical Recipes in FORTRAN, 2nd edn. Cambridge University Press, New York (1992)
Proga, D., Zhang, B.: Mon. Not. R. Astron. Soc. **370**, L61 (2006)
Qin, Y.P., et al.: Astrophys. J. **632**, 1008 (2005)
Ramirez-Ruiz, E., Fenimore, E.E.: Astrophys. J. **539**, 712 (2000)
Romano, et al.: Astron. Astrophys. **450**, 59 (2006)
Sari, R., Piran, T., Narayan, R.: Astrophys. J. **497**, L17 (1998)
Shenoy, A., et al.: Astrophys. J. **778**, 3 (2013)
Sonbas, E., et al.: Astrophys. J. **767**, L28 (2013)
Swenson, C., et al.: Astrophys. J. **774**, 2 (2013)
Wang, K., Dai, Z.: Astrophys. J. **772**, 152 (2013)
Willingale, R., Genet, F., Granot, J., et al.: Mon. Not. R. Astron. Soc. **403**, 1296 (2010)
Wu, X.F., et al.: (2005). astro-ph/0512555
Zhang, F.W., Qin, Y.P., Zhang, B.B.: Publ. Astron. Soc. Jpn. **59**, 857 (2007)
Zhang, F.W., Qin, Y.P.: New Astron. **13**, 485 (2008)
Zhang, F.W.: Astrophys. J. **685**, 1052 (2008)
Zhang, B., et al.: Astrophys. J. **642**, 354 (2006)